Estimation of Battery Parameters in Cascaded Half-Bridge Converters with Reduced Voltage Sensors

Nima Tashakor, Bita Arabsalmanabadi, Elham Hosseini, Kamal Al-Haddad, Stefan Goetz
Technische Universität Kaiserslautern
Kaiserslautern, Germany
E-Mail: Tashakor@eit.uni-kl.de

Acknowledgements

The authors acknowledge the financial support by the Federal Ministry of Education and Research of Germany in the project “Open6GHub” (grant number: 16KISK004).

Keywords

Modular battery, parameter estimation, modular multilevel converter

Abstract

Although modular multilevel converters (MMC) and cascaded half-bridge (CHB) converters are an established concept in HVDC, MMCs and CHBs have started to find new applications, including modular converters with integrated energy storage systems. Despite various advantages of the low-voltage modularity, a complex and expensive monitoring/control system can hinder finding a foothold in many emerging applications that are more cost-driven, such as the e-mobility market. Estimators and observers can reduce the monitoring cost and complexity by reducing the number of required sensors and communication bandwidth. However, estimation methods rarely consider MMCs with integrated battery, and most available methods neglect all resistances. This paper fills this gap by developing an online estimation technique for parameters of all battery modules in an MMC. The proposed method exploits the slow dynamics of the battery to use a simpler and less computationally demanding algorithm that can easily be implemented in low-end controllers. Based on the developed model of the system, the iterative algorithm can estimate the voltage and internal resistance of every module through measuring the output voltage and current of the battery pack and avoid direct measurements from the modules. As a result of substantial reduction in the number of monitoring sensors for estimating the battery parameters, the proposed technique is simpler and less costly in comparison with other sensor-based techniques. Furthermore, the proposed technique accelerates convergence using optimal learning rate value. Simulations validate the ability of the proposed estimation technique under different scenarios. The estimation technique can identify both internal resistance and open-circuit voltage of the batteries with approximately 2 % accuracy.

Introduction

As an alternative to conventional fuel, electric transportation has been growing rapidly over the last ten years. One of the main challenges in electric vehicles (EV) arises from the range anxiety [1]. Energy storage systems, usually batteries, are of paramount importance to address this issue by decreasing refilling time and increasing the capacity [2]. In addition, the introduction of fast and ultra-fast electric vehicle chargers increased the required voltage and power levels in an EV [3]. Correspondingly, the EV battery size has increased to hundreds of battery cells including multiple serial/parallel strings in each EV, which cannot be considered as one battery pack anymore, but rather a collection of modules hard-wired together [3]. While manufacturers use larger and larger batteries in cars, hot debates concerning the battery design and monitoring become more significant [4]. Experts believe that fully controlled modular batteries are the next step in the evolution of battery pack design with very high expectations for modular multilevel converters (MMC) and cascaded bridge converters (CBC) [5-10].

MMCs are dominate in high-voltage applications due to simplicity and cost-effectiveness; however, with the falling cost of power electronics, it is expected that their popularity also grows in medium- and low-voltage applications [11, 12]. One major trend in MMCs is to replace the capacitor of each module in a string with a battery, resulting in a fully controlled modular converter/battery pack and similar to normal MMCs. Multiple strings can be connected to form different dc, single-phase, and multi-phase structures [13]. Additionally, on the module level, MMCs can use different topologies, among which half-bridge (HB) is the most popular one at the moment [14, 15]. Requiring only two switches within each module offers the simplest circuit among several alternatives [16, 17]. Although an MMC with battery modules can offer many advantages, it requires constant monitoring of the module's states to ensure a balanced operation. The inherent tolerance of the modules and different thermal or load conditions as well as different aging factors can lead to charge imbalance among the modules [18, 19]. Imbalance between different modules is one of the main issues in any battery system including a modular one, which leads to shorter battery lifetime, lower accessible energy, and lower system efficacy [20, 21]. Therefore, the capacitors or batteries must be monitored constantly to ensure stable operation [22].

Most conventional monitoring systems rely on real-time measurements of each module's parameters [23]. However, in a high-power industrial application with a high number of modules, the collection and processing of all this data is a significant challenge [24, 25]. Additionally, multiple sensors per module increase cost and size of data acquisition system. Minimizing direct measurement of module capacitor voltages has been widely investigated in the recent literature by incorporating observers and estimators of those voltages [26-28]. Abushafa et al. use an exponentially weighted recursive least square technique to estimate the module capacitor voltages with only one voltage sensor per arm [26]. Arco et al. present an algorithm based on the operation of a two-step predictor–corrector scheme, where in the first step the algorithm uses a simple model-based estimation and then corrects the estimation based on the output voltage of the whole string in the second step [27]. The adaptive linear neuron algorithm ([28, 29]) and Kalman filter ([30, 31]) are other types of estimator with varying degree of accuracy that require only the output voltage of the string to estimate the voltage of every module. However, there are also models that focus on reducing the sensors throughout the string rather completely removing them. Rong et al. present a voltage estimation method that compensates the sampling delay effect [32]. The presented method divides the modules into groups and then estimates the capacitor voltages inside each group from the measured output voltage of the group. While most of the above-mentioned methods consider identical capacitor values, Taffese et al. propose an online voltage observer that considers both capacitance variation and time delay [33]. Konstantinou et al. provide a review of the different estimation/observation methods for MMCs [34].

Most of the reported techniques are applied to capacitor-based modules but are also applicable to battery-based modules to estimate the terminal voltage of the batteries. However, whereas the internal resistance of the capacitors is negligible, the internal resistance of the batteries is considerably higher and cannot be neglected [35]. Furthermore, although the terminal voltage of the battery is a particularly good indicator of its charge, this is not the case for batteries [36, 37]. Therefore, even though a wide range of techniques is available for estimating terminal voltage of the modules in MMC, to the best of our knowledge, none of them is able to estimate the internal and the open-circuit voltage of the battery modules, which are crucial in battery management and monitoring functions, such as state of charge and state of health monitoring [37-39]. Another noticeable difference between capacitors and batteries as the energy storage of a module is their dynamics. The voltage of a capacitor changes continuously with fairly fast dynamics, requiring estimators with high convergence speed and fast update rates. However, the battery parameters enjoy a slower dynamic, which can be exploited to reduce the estimator complexity using simpler methods [40].

This paper presents an estimation technique for open-circuit voltage and internal resistance of battery modules in an MMC topology. The proposed method decouples the equations of voltage and resistance through consecutive sampling of the output voltage and current of the pack and then proceeds with updating the voltage and resistance vectors. Furthermore, the learning factor of the system is optimized to minimize the convergence speed. The proposed technique benefits from low computation that can be implemented in most low-end controllers, without any additional sensor for the modules. Moreover, it has the advantage of estimating the internal resistance of the battery, which has previously been neglected.

The proposed MMC Structure

Figure 1 depicts the topology of a dc modular battery structure consisting of N half-bridge battery-based modules, inductor L, capacitor C, and the load/supply. The output voltage and current of the pack are measured using two sensors with the sampling time T_s. Each module includes a battery and two MOSFETs (i.e., $S_{i\mathrm{U}}$ and $S_{i\mathrm{L}}$) as well as their body diodes (i.e., $D_{i\mathrm{U}}$ and $D_{i\mathrm{L}}$). The modular system is a multilevel dc/dc bidirectional converter, behaving as a buck converter during discharge and a boost converter during charge.

A. Module Operating Modes

As Fig. 2 shows, each module contains a half-bridge and a battery, with four possible operation modes during bidirectional energy transfer as follows: i) $S_{1\mathrm{U}}$ is on, $S_{1\mathrm{L}}$ is off, and the batteries are charging. The terminal voltage of the battery is $v_{t_i} = V_{oc_i} - (r_{bt_i} + r_{dU_i})i_p$ (see Fig. 2(a), Mode 1); ii) $S_{1\mathrm{U}}$ is off, $S_{1\mathrm{L}}$ is on, and the batteries are charging. The module is bypassed, and the terminal voltage of the battery is $v_{t_i} = -r_{dsL_i}i_p$ (see Fig. 2(a), Mode 2); iii) $S_{1\mathrm{U}}$ is on, $S_{1\mathrm{L}}$ is off, and the batteries are discharging. The terminal voltage of the battery is $v_{t_i} = v_{oc_i} - (r_{bt_i} + r_{dsU_i})i_p$ (see Fig. 2(a), Mode 3); iv) $S_{1\mathrm{U}}$ is off, $S_{1\mathrm{L}}$ is on, and the batteries are discharging. The module is bypassed, and the terminal voltage of the battery is $v_{t_i} = -r_{dL_i}i_p$ (see Fig. 2(a), Mode 4).

For the sake of simplicity, we assume identical resistances for the MOSFETs and their body diodes. Consequently, Fig. 2(b) shows the electrical equivalent circuit of the battery when modules is connected in series to the arm and Fig. 2(c) shows the electrical equivalent circuit when the module is bypassed from the arm.

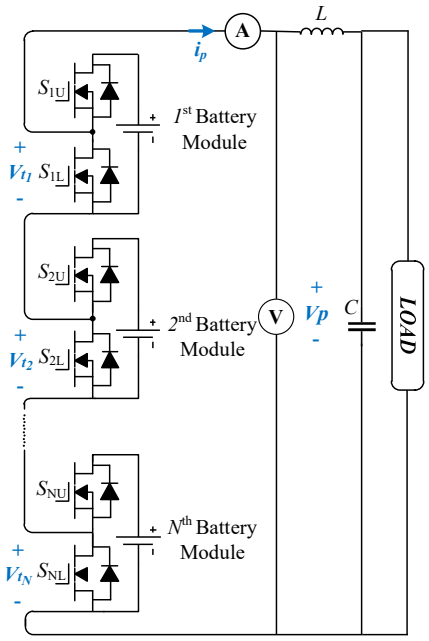

Fig.1 A single arm battery-based dc MMC macro structure

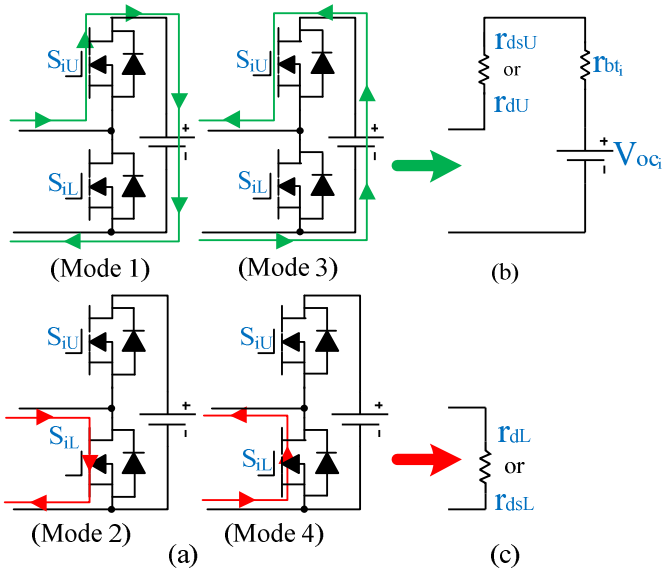

Fig. 2 The module structure (a) different operation modes of each module, (b) electrical equivalent model of a module when inserted in series (c) electrical equivalent of the module when bypassed.

B. Modulation Techniques

While there are many modulation techniques for MMCs, phase-shifted carrier (PSC) modulation is popular because of its stable performance during dynamic changes and ease of implementation [41]. In PSC modulation, the zero point of each carrier is slightly shifted with respect to its neighboring carriers, where the phase-shift of the j^{th} module follows $\varphi_i = 2\pi/N$. The switching signals result from comparing carrier waves with the with the modulation index. Figure 3 provides an intuitive representation of the MMC operation, where at first module two is discharging in Fig. 3(a) and then bypassed in Fig. 3(b). Additionally, Figure 3(c) shows the implementation of PSC modulation.

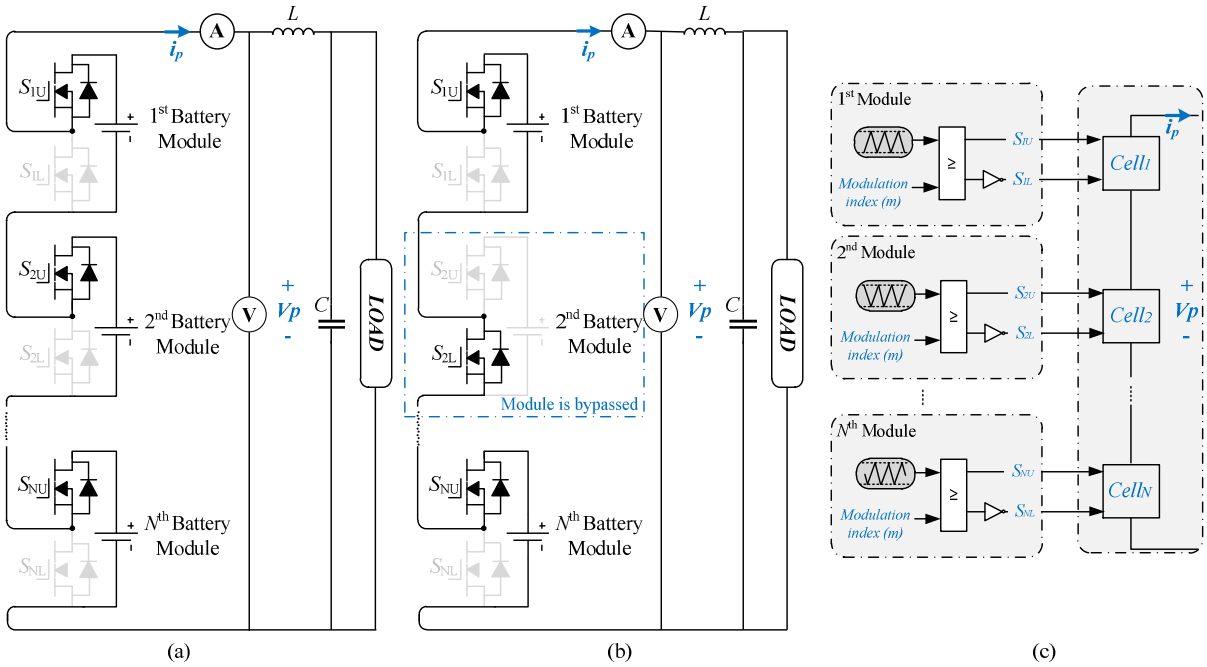

Fig.3 (a) all modules are in series; (b) the second modules is bypassed (c) Overall control block diagram of PSC modulation

Battery Parameter Estimation

In this paper, we propose an iterative algorithm to estimate parameters of each battery module in the battery-based MMC shown in Fig. 1. Using the developed mathematical model in the previous section, the proposed estimator–corrector algorithm can estimate the voltage and internal resistance of each module through measuring only the output voltage and current of the battery pack. Most of the existing reports consider battery as a single DC source with negligible resistance. The technique is the same for both voltage and resistance estimation.

As discussed, there is a nonlinear relation between the system parameters. A BP parameter estimation algorithm is derived to estimate battery parameters in the proposed non-linear dynamic model. As shown in Fig. 6, an error function is defined between the measured and the model outputs.

A. Mathematical model of the MMC

Figure 4 depicts the equivalent model of one arm. We can model the battery in its simplest form with a constant voltage source as the open-circuit voltage in series with a resistance. The open-circuit voltage depends on the battery's state of charge, but for the purpose of modeling, it can be considered constant in brief intervals. In Fig. 4, R_{eq} depicts the effective resistance of the entire arm. The KVL on the arm results in (1.a) and (1.b) for charge and discharge states respectively.

$$v_p(t) = \left(\boldsymbol{S_U}(t)\right)^T \boldsymbol{V_{OC}} - i_p(t)\begin{bmatrix}\left(\boldsymbol{S_U}(t)\right)^T\left(\boldsymbol{R_{bt}} - \boldsymbol{R_{ds,U}}\right)\\ -\left(\boldsymbol{S_L}(t)\right)^T \boldsymbol{R_{d,L}}\end{bmatrix} \quad (1.a)$$

$$v_p(t) = (\boldsymbol{S_U}(t))^T \boldsymbol{V_{OC}} - i_p(t)\begin{bmatrix}\left(\boldsymbol{S_U}(t)\right)^T\left(\boldsymbol{R_{bt}} - \boldsymbol{R_{d,U}}\right)\\ -(\boldsymbol{S_L}(t))^T \boldsymbol{R_{ds,L}}\end{bmatrix} \quad (1.b)$$

where $\boldsymbol{S_U}$ and $\boldsymbol{S_L}$ are the vectors of gate signals for the upper switches and lower switches. $\boldsymbol{R_{ds}}$ and $\boldsymbol{R_d}$ are respectively the switch and diode resistances' vectors, where the subscripts U and L correspond to upper and lower switches in

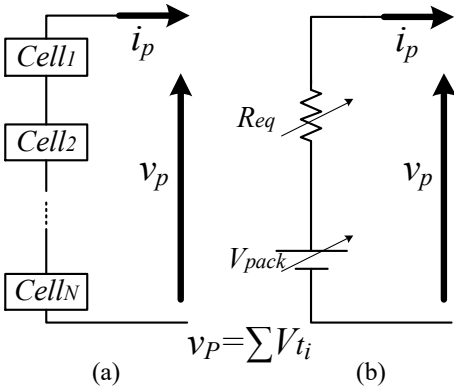

Fig.4. MMC circuit and associated current dynamic loops: (a) Converter schematic. (b) Equivalent circuit of output current and voltage

the half-bridges. Furthermore, $\boldsymbol{V_{OC}}$ and $\boldsymbol{R_{bt}}$ correspond to the open-circuit voltages and internal resistances of the modules. v_p and i_p are the measured voltage and current of the pack terminals. Also, as shown in Fig. 4, the positive direction of the pack current is during discharging. For the sake of simpler representation, we consider the resistances of lower and upper MOSFETs as well as diodes equal, i.e., $\boldsymbol{R_{ds,U}} = \boldsymbol{R_{ds,L}} = \boldsymbol{R_{d,U}} = \boldsymbol{R_{d,L}} = \boldsymbol{R_{sw}}$. Therefore, we can further simplify (1) in discrete time domain as

$$v_p^{(k)} = \boldsymbol{S_U^{(k)}} \times \boldsymbol{V_{oc}} - i_p^{(k)}.\left[\left(\boldsymbol{S_U^{(k)}}\right)^T \times \boldsymbol{R_{bt}} + \left(\boldsymbol{S_U^{(k)}} + \boldsymbol{S_L^{(k)}}\right)^T \times \boldsymbol{R_{sw}}\right], \tag{2}$$

where subscripts k shows the k^{th} sample.

Additionally, $\boldsymbol{S_U^{(k)}}$ and $\boldsymbol{S_L^{(k)}}$ are complementary, and the resultant vector of $\boldsymbol{S_U^{(k)}} + \boldsymbol{S_L^{(k)}}$ is a unity vector. Hence, (2) can be further simplified to

$$v_p^{(k)} = \boldsymbol{S_U^{(k)}} \times \boldsymbol{V_{oc}} - i_p^{(k)}.\left[\left(\boldsymbol{S_U^{(k)}}\right)^T \times \boldsymbol{R_{bt}} + Nr_{sw}\right], \tag{3}$$

where r_{sw} is the internal resistance of one switch/diode and the total number of modules is N.

As can be seen, both $\boldsymbol{R_{bt}}$ and $\boldsymbol{V_{oc}}$ can affect the output of the pack. Therefore, it is necessary to somehow decouple the effect of these two vectors in (3). With that goal in mind, we write (3) for two consecutive instances of k and $(k+1)$ as follows

$$v_p^{(k)} + i_p^{(k)}.N.r_{sw} = \left(\boldsymbol{S_U^{(k)}}\right)^T \times \boldsymbol{V_{oc}} - i_p^{(k)}.\left(\boldsymbol{S_U^{(k)}}\right)^T \times \boldsymbol{R_{bt}}, \tag{4}$$

$$v_p^{(k+1)} + i_p^{(k+1)}.N.r_{sw} = \left(\boldsymbol{S_U^{(k+1)}}\right)^T \times \boldsymbol{V_{oc}} - i_p^{(k+1)}.\left(\boldsymbol{S_U^{(k+1)}}\right)^T \times \boldsymbol{R_{bt}}. \tag{5}$$

Subtracting (4) from (5) when $\boldsymbol{S_U^{(k)}} = \boldsymbol{S_U^{(k+1)}} = \boldsymbol{S_U}$, we can remove V_{oc} from the new equations per

$$\Delta v_p + \Delta i_p.N.r_{sw} = -\Delta i_{pack}.(\boldsymbol{S_U})^T \times \boldsymbol{R_{bt}}, \tag{6}$$

where $\Delta v_p = v_p^{(k+1)} - v_p^{(k)}$; and $\Delta i_p = i_p^{(k+1)} - i_p^{(k)}$. By doing so, $\boldsymbol{V_{oc}}$ is removed from the equation and R_{bt} is the only variant. We can rewrite (6) as

$$-\frac{\Delta v_p}{\Delta I_p} - N.r_{sw} = (\boldsymbol{S_U})^T \times \boldsymbol{R_{bt}}. \tag{7}$$

With $\boldsymbol{R_{bt}}$ as the only variable in (7), we can use a back propagation algorithm to solve it [28]. In this step, iterative methods can estimate $\boldsymbol{R_{bt}}$ using

$$\boldsymbol{W_1^{(k+1)}} = \boldsymbol{W_1^{(k)}} + \alpha_1\, \boldsymbol{x}(y_1 - \hat{y}_1), \tag{8}$$

where α_1 is learning rate, and k and $(k+1)$ denote the present and next samples, respectively. Also, $y_1 = -\frac{\Delta v_p}{\Delta I_p} - Nr_{sw}$, $\hat{y}_1 = (\boldsymbol{S_U})^T \times \boldsymbol{R_{bt}}$, and $\boldsymbol{x} = \boldsymbol{S_U} \times \boldsymbol{W_1^{(k+1)}}$ is the updated estimate of the internal resistance vector ($\boldsymbol{R_{bt}}$) and $\boldsymbol{W_1^{(0)}}$ the initial estimate. The vector of internal resistance (R_{bt}) is updated in each-time step based on (8) under the condition that $\boldsymbol{S_U^{(k)}} = \boldsymbol{S_U^{(k+1)}}$. If the $\boldsymbol{S_U^{(k)}} \neq \boldsymbol{S_U^{(k+1)}}$ then the $\boldsymbol{R_{bt}}$ retains its previous value. In the next step, the vector of open-circuit voltages $\boldsymbol{V_{oc}}$ is updated through a similar procedure, either using the new $\boldsymbol{R_{bt}}$ or using its old value. Equation (3) can be rewritten as

$$v_p^{(k+1)} + i_p^{(k+1)}\left(\boldsymbol{S_U^{(k+1)}}\right)^T \times \boldsymbol{R_{bt}} + Nr_{sw} = \left(\boldsymbol{S_U^{(k+1)}}\right)^T \times \boldsymbol{V_{oc}}. \tag{9}$$

Similar to the procedure for updating the internal resistance vector, $\boldsymbol{V_{oc}}$ vector is estimated using

$$\boldsymbol{W_2^{(k+1)}} = \boldsymbol{W_2^{(k+1)}} + \alpha_2 \boldsymbol{x}(y_2 - \hat{y}_2), \tag{10}$$

where α_2 is the learning rate, $y_2 = v_p^{(k+1)} + i_p^{(k+1)} \left(\boldsymbol{S_U^{(k+1)}}\right)^T \times \boldsymbol{R_{bt}} + N r_{sw}$, $\hat{y}_2 = \left(\boldsymbol{S_U^{(k+1)}}\right)^T \boldsymbol{V_{oc}}$, $\boldsymbol{x} = \boldsymbol{S_U^{(k+1)}}$, and $\boldsymbol{W_2^{(k+1)}}$ is the updated vector of open-circuit voltages of the batteries.

The convergence speed of (8) and (10) is determined according to the learning rate. To optimize the convergence speed, a line search algorithm is used to optimize the value of the learning rates α_1 and α_2. The details of optimizing the learning rate using the line search algorithm are presented in Appendix I and II. Based on the optimization results, the optimum learning rates that result into the fastest convergence for (8) and (10) are identical and equal to $\alpha_1 = \alpha_2 = \frac{1}{\boldsymbol{x}^T \boldsymbol{x}}$. Therefore, the optimum estimators are

$$\begin{cases} \boldsymbol{W_{1,k+1}} = \boldsymbol{W_{1,k}} + \boldsymbol{x}^T \frac{(y_2 - \hat{y}_2)}{x\, x^T}, \\ \boldsymbol{W_{2,k+1}} = \boldsymbol{W_{2,k}} + \boldsymbol{x}^T \frac{(y_2 - \hat{y}_2)}{\boldsymbol{x} \times \boldsymbol{x}^T}. \end{cases} \tag{11}$$

After updating both $\boldsymbol{R_{bt}}$ and $\boldsymbol{V_{oc}}$, the pack voltage is estimated using (3) and compared to the actual measurement, in case the difference is lower than a minimum threshold, the estimator has converged, and the values are usable.

Figure 5 presents the flowchart of the proposed decoupling and estimation method. Based on the algorithm flowchart, the controller receives two consecutive samples (k) and $(k+1)$ of pack voltage and current as well as the switching states of the modules. If the controller receives identical switching states and detects a variation in current, then the controller will update the previous estimation of the internal resistance vector according to (8), otherwise this step is skipped. Then the controller updates the vector of open-circuit voltages using (10) and goes to the beginning of the algorithm. When the output voltage estimation of the pack is close to the measured value for more than N iterations, then we can conclude that the estimator has converged to its final values.

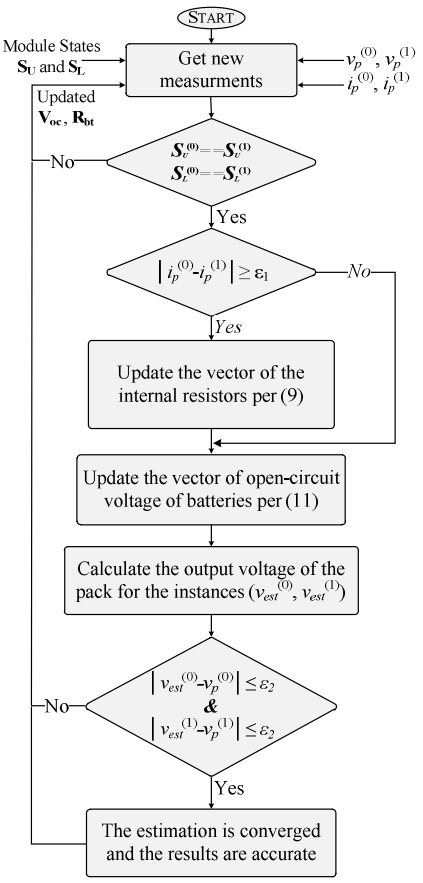

Fig. 5. The proposed back-propagation algorithm

Results and Discussions

Detailed simulations in MATLAB/Simulink study the performance of the proposed estimation technique using a single-arm modular battery system. Table I provides the main parameters of the simulated system, with eight half-bridge modules. In the simulation, batteries are modelled using a simplified electrical equivalent circuit consisting of an internal resistance as well as a constant dc voltage source. The modular battery is feeding a resistive load.

Fig. 6 (a) and (b) present the output voltage and current of the battery pack as well as the load. At $t = 0.25$ s, the modulation index is changed from 0.4 to 0.8. Figure 7 depicts the results of the average estimation error for output voltage and internal resistance of battery cells and the estimation results of output voltage and internal resistance of battery cells for all modules during ideal condition. We consider ideal condition to be the condition where all the modules have identical parameters. While the actual internal resistance of all modules is 5 mΩ, the estimation vector is initialized with every resistance equal to

Table I Parameters of single arm MMC

PARAMETER	VALUE
V_{dc}	$400-800\ [V]$
C_{dc}	$10\ [\mathrm{m}F]$
L_{dc}	$1\ [\mathrm{m}H]$
R_{ldc}	$10\ [\mathrm{m}\Omega]$
R_{load}	$3.2\ [\Omega]$
R_{ds}	$1\ [\mathrm{m}\Omega]$
R_d	$1\ [\mathrm{m}\Omega]$
$v_{oc,1-8}$	$120\ [V]$
$r_{bt,1\sim8}$	$5\ [\mathrm{m}\Omega]$

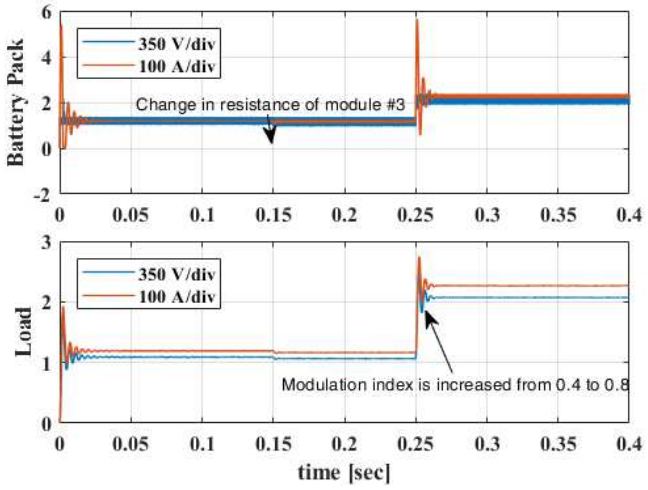

Fig. 6 (a) The output voltage and current of battery pack (b) The output voltage and current of load

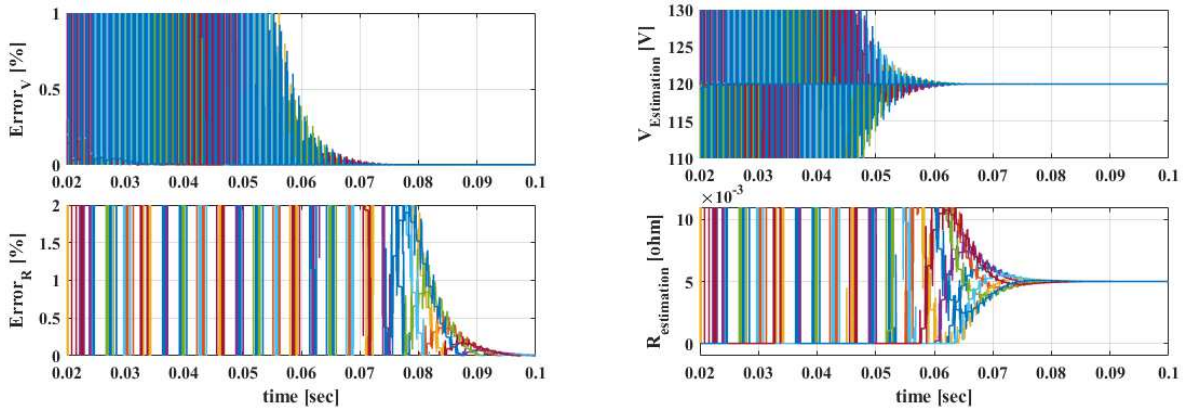

(a) (b)

Fig. 7 simulation results for ideal conditions(a) estimation errors; (b) estimation values for open-circuit voltage and internal resistance of battery modules

1 Ω. Consequently, the error is significant at the beginning. However, once the estimator is activated, it converges in less than 90 ms.

Figure 8(a) illustrates the behavior of the estimator when the internal resistance of one module is changed to 0.1 Ω to simulate an abnormal condition. The resistance of module three is changed at $t = 0.2$ s and Fig. 8(b) show that the estimation vector converges to correct values in 5 ms. The results validate the accuracy and high speed of the proposed algorithm which is proper for industrial

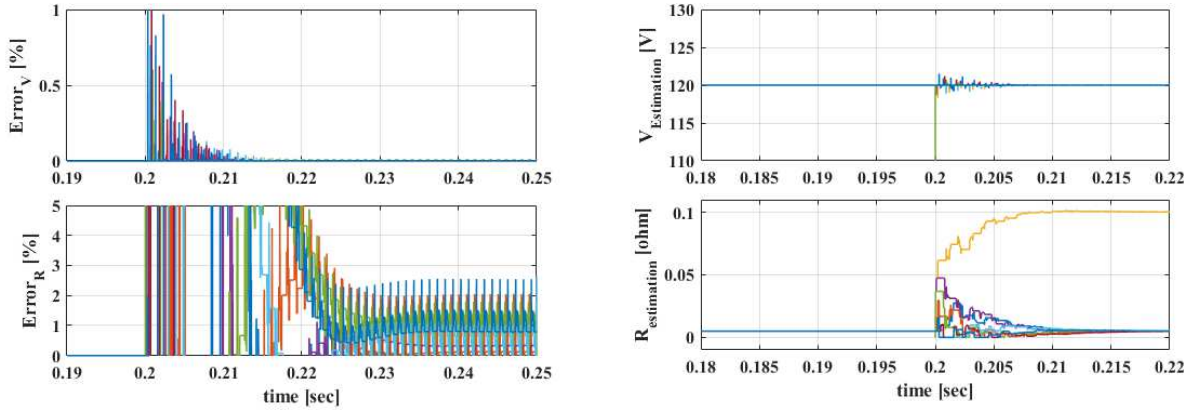

(a) (b)

Fig. 8 simulation results for abnormal conditions(a) estimation errors; (b) estimation values for open-circuit voltage and internal resistance of battery modules

applications.

Conclusions

This paper presents a decoupling technique as well as a back-propagation algorithm to estimate open-circuit voltage and internal resistance battery-based modules in a modular battery system. The proposed estimation technique exploits the already available data about the output voltage and current of the pack as well as the switching states of the modules and requires no extra measurement for estimation purposes. The line search optimization maximizes the convergence speed of the algorithm, which is confirmed through simulations. The proposed technique benefits from low-cost implementation as it requires fewer sensors and little computation. Furthermore, the proposed estimation algorithm can be easily extended for modular battery systems with several arms.

APPENDIX I

To have the maximum speed of convergence for estimating R_{bt}, an optimization function $C_1\left(R_{bt}^{(k)}\right)$ is defined based on a least square scheme to calculate the difference between $y_1 = -\frac{\Delta V_p}{\Delta I_p} - Nr_{sw}$, and $\hat{y}_1 = (S_U)^T R_{bt}$ as

$$C_1\left(R_{bt}^{(k)}\right) = \frac{1}{2}\left[(S_U)^T R_{bt}^{(k)} + \frac{\Delta v_p}{\Delta i_p} + Nr_{sw}\right]^2. \quad (12)$$

Gradient of $C_1(R_{bt}^{(k)})$ over $R_{bt}^{(k)}$ is presented by $S^{(k)}$as

$$S^{(k)} = -\nabla C_1 = -S_U\left((S_U)^T R_{bt}^{(k)} + A_1\right), \quad (13)$$

where $A_1 = \frac{\Delta v_o^{(k)}}{\Delta i_o^{(k)}} + Nr_{sw}$. We can use $S^{(k)}$ to update $R_{bt}^{(k)}$ in the direction that reduces the error (i.e., reduces $C_1(R_{bt})$) as follows

$$R_{bt}^{(k+1)} = R_{bt}^{(k)} + \alpha_1^{(k)} S^{(k)}. \quad (14)$$

The value of α_1 determines the convergence speed and to achieve maximum convergence speed we will use the exact line search algorithm for optimizing the value of α_1. Using the gradient of $C_1(R_{bt}^{(k+1)})$ over α_1 and equating it with zero results into

$$C_1'^{(k+1)}(\alpha^*) = \nabla C_1\left(R_{bt}^{(k)} + \alpha^* S^{(k)}\right)^T S^{(k)} = 0, \quad (15)$$

where α_1^* is the optimum value for α_1.

By substituting (12) and (14), we can rewrite (15) per

$$\left[(S_U)^T\left(R_{bt}^{(k)} + \alpha^* S^{(k)}\right) + A_1\right]^T (S_U)^T\left[S_U\left((S_U)^T R_{bt}^{(k)} + A_1\right)\right] = 0. \quad (16)$$

Substituting (13) in (16) results in

$$\left[(S_U)^T R_{bt}^{(k)} + \alpha^* (S_U)^T\left(-S_U\left((S_U)^T R_{bt}^{(k)} + A_1\right)\right) + A_1\right]^T (S_U)^T\left[S_U\left((S_U)^T R_{bt}^{(k)} + A_1\right)\right] = 0. \quad (17)$$

After some simplifications and rearrangements, (17) turns into

$$\left[(S_U)^T R_{bt}^{(k)} - \alpha^* (S_U)^T S_U\left((S_U)^T R_{bt}^{(k)} + A_1\right) + A_1\right]^T (S_U)^T S_U\left((S_U)^T R_{bt}^{(k)} + A_1\right) = 0, \quad (18)$$

which can be solved for α^* per

$$\alpha^* = \frac{1}{(S_U)^T S_U}. \tag{19}$$

APPENDIX II

To have the maximum speed of convergence to estimate V_{oc}, an optimization function $C_1\left(V_{oc}^{(k)}\right)$ is defined based on least square technique to calculate the difference between $y_2 = v_p^{(k)} + i_p^{(k)}\left[(S_U)^T R_{bt}^{(k)} + N r_{sw}\right]$, and $\hat{y}_2 = S_U V_{oc}^{(k)}$ as

$$C_2\left(V_{oc}^{(k)}\right) = \frac{1}{2}\left[v_p^{(k)} + i_p^{(k)} R_{eq2} - (S_U)^T V_{oc}^{(k)}\right]^2, \tag{20}$$

where $R_{eq2} = (S_U)^T R_{bt} + N r_{sw}$. Similar to Appendix I, gradient of $C_1(V_{oc}^{(k)})$ over $V_{oc}^{(k)}$ is represented by $S^{(k)}$as follows

$$S^{(k)} = -\nabla C_2 = -S_U^T \left(A_2 - (S_U)^T V_{oc}^{(k)}\right), \tag{21}$$

where $A_2 = v_p^{(k)} + i_p^{(k)} R_{eq2}$. Therefore, the vector of the open-circuit voltages can be updated using

$$V_{bt}^{(k+1)} = V_{oc}^{(k)} + \alpha^{(k)} S^{(k)}. \tag{22}$$

Similarly, the exact line search algorithm can be used to find the optimum value of the learning rate α_2. Gradient of $C_2(V_{oc}^{(k+1)})$ over α_2 is

$$\nabla C_2 \left(V_{oc}^{(k+1)}\right)^T S^{(k)} = 0. \tag{23}$$

Replacing (22) and (23) in (24) results into

$$\left[-S_U A_2 + S_U (S_U)^T \left[V_{oc}^{(k)} - \alpha^* S_U \left(A_2 - (S_U)^T V_{oc}^{(k)}\right)\right]\right]^T \left[S_U \left(A_2 - (S_U)^T V_{oc}^{(k)}\right)\right] = 0. \tag{24}$$

With some simplifications, (24) is rearranged into

$$(S_U)^T \left[-A_2 + (S_U)^T V_{oc}^{(k)} + \alpha^* (S_U)^T S_U \left(A_2 - (S_U)^T V_{oc}^{(k)}\right)\right] \left[A_2 - (S_U)^T V_{oc}^{(k)}\right] S_U = 0, \tag{25}$$

which has two roots per

$$\begin{cases} A_2 = (S_U)^T V_{oc}^{(k)} \\ -A_2 + (S_U)^T V_{oc}^{(k)} + \alpha^* (S_U)^T S_U \left(A_2 - (S_U)^T V_{oc}^{(k)}\right) = 0 \end{cases}. \tag{26}$$

While one of the roots is independent of α_2 and only happens if the estimator is converged to the exact open-circuit voltage, the other one can be solved for α_2 per

$$\alpha^* = \frac{1}{(S_U)^T S_U}. \tag{27}$$

References

[1] N. Tashakor, V. Monteiro, T. Ghanbari, and E. Farjah, "An Improved Modular Charge Equalization Structure for Series Cascaded Battery," presented at the 2019 27th Iranian Conference on Electrical Engineering (ICEE), 30 April-2 May 2019, 2019.

[2] A. N. Link, O'Connor, A. C., Scott, T. J., "Battery Technology for Electric Vehicles.," *London: Routledge, ,* 2015, doi: https://doi.org/10.4324/9781315749303.

[3] C. Jung, "Power Up with 800-V Systems: The benefits of upgrading voltage power for battery-electric passenger vehicles," *IEEE Electrification Magazine,* vol. 5, no. 1, pp. 53-58, 2017, doi: 10.1109/MELE.2016.2644560.
[4] J. Fang, Y. Tang, H. Li, and X. Li, "A Battery/Ultracapacitor Hybrid Energy Storage System for Implementing the Power Management of Virtual Synchronous Generators," *IEEE Transactions on Power Electronics,* vol. 33, no. 4, pp. 2820-2824, 2018, doi: 10.1109/TPEL.2017.2759256.
[5] M. Gjelaj, S. Hashemi, C. Traeholt, and P. B. Andersen, "Grid integration of DC fast-charging stations for EVs by using modular li-ion batteries," *IET Generation, Transmission & Distribution,* vol. 12, no. 20, pp. 4368-4376, 2018, doi: 10.1049/iet-gtd.2017.1917.
[6] S. M. Goetz, Z. Li, A. V. Peterchev, X. Liang, C. Zhang, and S. M. Lukic, "Sensorless scheduling of the modular multilevel series-parallel converter: enabling a flexible, efficient, modular battery," presented at the 2016 IEEE Applied Power Electronics Conference and Exposition (APEC), 2016.
[7] M. Quraan, P. Tricoli, S. D'Arco, and L. Piegari, "Efficiency assessment of modular multilevel converters for battery electric vehicles," *IEEE Transactions on Power Electronics,* vol. 32, no. 3, pp. 2041-2051, 2016.
[8] C. Gan, Q. Sun, J. Wu, W. Kong, C. Shi, and Y. Hu, "MMC-Based SRM Drives With Decentralized Battery Energy Storage System for Hybrid Electric Vehicles," *IEEE Transactions on Power Electronics,* vol. 34, no. 3, pp. 2608-2621, 2019, doi: 10.1109/TPEL.2018.2846622.
[9] N. Tashakor, E. Farjah, and T. Ghanbari, "A Bidirectional Battery Charger With Modular Integrated Charge Equalization Circuit," *IEEE Transactions on Power Electronics,* vol. 32, no. 3, pp. 2133-2145, 2017, doi: 10.1109/TPEL.2016.2569541.
[10] J. Fang, S. Yang, H. Wang, N. Tashakor, and S. Goetz, "Reduction of MMC capacitances through parallelization of symmetrical half-bridge submodules," *IEEE Transactions on Power Electronics,* 2021.
[11] M. Priya, P. Ponnambalam, and K. Muralikumar, "Modular-multilevel converter topologies and applications – a review," *IET Power Electronics,* vol. 12, no. 2, pp. 170-183, 2019, doi: 10.1049/iet-pel.2018.5301.
[12] J. Fang, H. Deng, N. Tashakor, F. Blaabjerg, and S. M. Goetz, "State-Space Modeling and Control of Grid-Tied Power Converters with Capacitive/Battery Energy Storage and Grid-Supportive Services," *IEEE Journal of Emerging and Selected Topics in Power Electronics,* pp. 1-1, 2021, doi: 10.1109/JESTPE.2021.3101527.
[13] Y. Li and Y. Han, "A Module-Integrated Distributed Battery Energy Storage and Management System," *IEEE Transactions on Power Electronics,* vol. 31, no. 12, pp. 8260-8270, 2016, doi: 10.1109/TPEL.2016.2517150.
[14] S. Gonzalez, Verne, S., Valla, M. , "Multilevel Converters for Industrial Applications," 2014, doi: 10.1201/b15252.
[15] D. Ronanki and S. S. Williamson, "Modular multilevel converters for transportation electrification: Challenges and opportunities," *IEEE Transactions on Transportation Electrification,* vol. 4, no. 2, pp. 399-407, 2018.
[16] Z. Li, R. Lizana, S. Sha, Z. Yu, A. V. Peterchev, and S. Goetz, "Module Implementation and Modulation Strategy for Sensorless Balancing in Modular Multilevel Converters," *IEEE Transactions on Power Electronics,* 2018.
[17] N. Tashakor, M. Kilictas, E. Bagheri, and S. Goetz, "Modular Multilevel Converter with Sensorless Diode-Clamped Balancing through Level-Adjusted Phase-Shifted Modulation," *IEEE Transactions on Power Electronics,* pp. 1-1, 2020, doi: 10.1109/TPEL.2020.3041599.
[18] A. Ghazanfari and Y. A. I. Mohamed, "A Hierarchical Permutation Cyclic Coding Strategy for Sensorless Capacitor Voltage Balancing in Modular Multilevel Converters," *IEEE Journal of Emerging and Selected Topics in Power Electronics,* vol. 4, no. 2, pp. 576-588, 2016, doi: 10.1109/JESTPE.2015.2460672.
[19] G. Chen, H. Peng, R. Zeng, Y. Hu, and K. Ni, "A Fundamental Frequency Sorting Algorithm for Capacitor Voltage Balance of Modular Multilevel Converter With Low-Frequency Carrier Phase Shift Modulation," *IEEE Journal of Emerging and Selected Topics in Power Electronics,* vol. 6, no. 3, pp. 1595-1604, 2018, doi: 10.1109/JESTPE.2017.2764684.
[20] X. Hui, F. Yatao, and W. Yiying, "Review of equalizing methods for battery pack," presented at the Electrical Machines and Systems (ICEMS), 2014 17th International Conference on, 22-25 Oct. 2014, 2014.
[21] T. Kacetl, J. Kacetl, N. Tashakor, M. Jaensch, and S. Goetz, "Degradation-Reducing Control for Dynamically Reconfigurable Batteries," *arXiv preprint arXiv:2202.11757,* 2022.
[22] N. Tashakor, B. Arabsalmanabadi, F. Naseri, and S. Goetz, "Low-Cost Parameter Estimation Approach for Modular Converters and Reconfigurable Battery Systems Using Dual-Kalman-Filter," *IEEE Transactions on Power Electronics,* pp. 1-1, 2021, doi: 10.1109/TPEL.2021.3137879.
[23] B. Arabsalmanabadi, N. Tashakor, Y. Zhang, K. Al-Haddad, and S. Goetz, "Parameter Estimation of Batteries in MMCs with Parallel Connectivity using PSO," presented at the IECON 2021 – 47th Annual Conference of the IEEE Industrial Electronics Society, 13-16 Oct. 2021, 2021.

[24]H. B. I, S. Rivera, Z. Li, S. Goetz, A. Peterchev, and R. L. F, "Different parallel connections generated by the Modular Multilevel Series/Parallel Converter: an overview," presented at the IECON 2019 - 45th Annual Conference of the IEEE Industrial Electronics Society, 14-17 Oct. 2019, 2019.
[25]N. Tashakor, Z. Li, and S. M. Goetz, "A Generic Scheduling Algorithm for Low-Frequency Switching in Modular Multilevel Converters with Parallel Functionality," *IEEE Transactions on Power Electronics,* pp. 1-1, 2020, doi: 10.1109/TPEL.2020.3018168.
[26]O. S. M. Abushafa, S. M. Gadoue, M. S. A. Dahidah, D. J. Atkinson, and P. Missailidis, "Capacitor Voltage Estimation Scheme With Reduced Number of Sensors for Modular Multilevel Converters," *IEEE Journal of Emerging and Selected Topics in Power Electronics,* vol. 6, no. 4, pp. 2086-2097, 2018, doi: 10.1109/JESTPE.2018.2797245.
[27] S. D. Arco and J. A. Suul, "Estimation of sub-module capacitor voltages in modular multilevel converters," in *2013 15th European Conference on Power Electronics and Applications (EPE)*, 2-6 Sept. 2013 2013, pp. 1-10, doi: 10.1109/EPE.2013.6631931.
[28] M. Abdelsalam, S. Tennakoon, H. Diab, and M. I. Marei, "An ADALINE based capacitor voltage estimation algorithm for modular multilevel converters," in *2016 19th International Symposium on Electrical Apparatus and Technologies (SIELA)*, 29 May-1 June 2016 2016, pp. 1-4, doi: 10.1109/SIELA.2016.7542968.
[29]P. Poblete, G. Pizarro, G. Droguett, F. Nunez, P. Judge, and J. Pereda, "Distributed Neural Network Observer for Submodule Capacitor Voltage Estimation in Modular Multilevel Converters," *IEEE Transactions on Power Electronics,* pp. 1-1, 2022, doi: 10.1109/TPEL.2022.3163395.
[30]M. D. Islam, R. Razzaghi, and B. Bahrani, "Arm-Sensorless Sub-Module Voltage Estimation and Balancing of Modular Multilevel Converters," *IEEE Transactions on Power Delivery,* vol. 35, no. 2, pp. 957-967, 2020, doi: 10.1109/TPWRD.2019.2931287.
[31]G. Pizarro, P. M. Poblete, G. Droguett, J. Pereda, and F. Nunez, "Extended Kalman Filtering for Full State Estimation and Sensor Reduction in Modular Multilevel Converters," *IEEE Transactions on Industrial Electronics,* pp. 1-1, 2022, doi: 10.1109/TIE.2022.3165286.
[32]F. Rong, X. Gong, X. Li, and S. Huang, "A New Voltage Measure Method for MMC Based on Sample Delay Compensation," *IEEE Transactions on Power Electronics,* vol. 33, no. 7, pp. 5712-5723, 2018, doi: 10.1109/TPEL.2017.2748969.
[33]A. A. Taffese, E. d. Jong, S. D'Arco, and E. Tedeschi, "Online Parameter Adjustment Method for Arm Voltage Estimation of the Modular Multilevel Converter," *IEEE Transactions on Power Electronics,* vol. 34, no. 12, pp. 12491-12503, 2019, doi: 10.1109/TPEL.2019.2907178.
[34] G. Konstantinou, H. R. Wickramasinghe, C. D. Townsend, S. Ceballos, and J. Pou, "Estimation Methods and Sensor Reduction in Modular Multilevel Converters: A Review," in *2018 8th International Conference on Power and Energy Systems (ICPES)*, 21-22 Dec. 2018 2018, pp. 23-28, doi: 10.1109/ICPESYS.2018.8626987.
[35]B. G. Carkhuff, P. A. Demirev, and R. Srinivasan, "Impedance-Based Battery Management System for Safety Monitoring of Lithium-Ion Batteries," *IEEE Transactions on Industrial Electronics,* vol. 65, no. 8, pp. 6497-6504, 2018, doi: 10.1109/TIE.2017.2786199.
[36]B. Arabsalmanabadi, N. Tashakor, A. Javadi, and K. Al-Haddad, "Charging Techniques in Lithium-Ion Battery Charger: Review and New Solution," presented at the IECON 2018 - 44th Annual Conference of the IEEE Industrial Electronics Society, 21-23 Oct. 2018, 2018.
[37]D. N. T. How, M. A. Hannan, M. S. H. Lipu, K. S. M. Sahari, P. J. Ker, and K. M. Muttaqi, "State-of-Charge Estimation of Li-ion Battery in Electric Vehicles: A Deep Neural Network Approach," *IEEE Transactions on Industry Applications,* pp. 1-1, 2020, doi: 10.1109/TIA.2020.3004294.
[38]C. R. Gould, C. M. Bingham, D. A. Stone, and P. Bentley, "New Battery Model and State-of-Health Determination Through Subspace Parameter Estimation and State-Observer Techniques," *IEEE Transactions on Vehicular Technology,* vol. 58, no. 8, pp. 3905-3916, 2009, doi: 10.1109/TVT.2009.2028348.
[39]X. Tan *et al.*, "Real-Time State-of-Health Estimation of Lithium-Ion Batteries Based on the Equivalent Internal Resistance," *IEEE Access,* vol. 8, pp. 56811-56822, 2020, doi: 10.1109/ACCESS.2020.2979570.
[40]O. S. H. M. Abushafa, M. S. A. Dahidah, S. M. Gadoue, and D. J. Atkinson, "Submodule Voltage Estimation Scheme in Modular Multilevel Converters with Reduced Voltage Sensors Based on Kalman Filter Approach," *IEEE Transactions on Industrial Electronics,* vol. 65, no. 9, pp. 7025-7035, 2018, doi: 10.1109/TIE.2018.2795519.
[41]N. Tashakor and M. Khooban, "An Interleaved Bi-Directional AC–DC Converter With Reduced Switches and Reactive Power Control," *IEEE Transactions on Circuits and Systems II: Express Briefs,* vol. 67, no. 1, pp. 132-136, 2020, doi: 10.1109/TCSII.2019.2903389.